Palaeogeography, Palaeoclimatology, Palaeoecology 514 (2019) 251–264

Contents lists available at ScienceDirect

Palaeogeography, Palaeoclimatology, Palaeoecology

journal homepage: www.elsevier.com/locate/palaeo

Drought (scPDSI) reconstruction of trans-Himalayan region of central Himalaya using *Pinus wallichiana* tree-rings

Narayan Prasad Gaire[a,b,c], Yub Raj Dhakal[c,d], Santosh K. Shah[e], Ze-Xin Fan[a,*], Achim Bräuning[f], Uday Kunwar Thapa[g], Sanjaya Bhandari[h], Suman Aryal[c,i], Dinesh Raj Bhuju[j]

[a] Key Laboratory of Tropical Forest Ecology, Xishuangbanna Tropical Botanical Garden, Chinese Academy of Sciences, Menglun, Mengla, Yunnan 666303, PR China
[b] GoldenGate International College, Battisputali, Kathmandu, Nepal
[c] Treering Society of Nepal, Lalitpur, Nepal
[d] Siddhartha Environmental Services, Kathmandu, Nepal
[e] Birbal Sahni Institute of Palaeosciences, Lucknow 226007, India
[f] Institute of Geography, University of Erlangen-Nürnberg, 91058 Erlangen, Germany
[g] Department of Geography, Environment and Society, University of Minnesota, Minneapolis, USA
[h] Department of Earth and Environmental System, Indiana State University, USA
[i] International Institute for Research, Education and Consultancy (IIREC), Queensland, Australia
[j] Nepal Academy of Science and Technology, Khumaltar, Lalitpur, Nepal

ARTICLE INFO

Keywords:
Climate change
Growth-climate response
Dendroclimatology
Dolpo
Drought
Nepal
Paleoclimatology
Ring width

ABSTRACT

Knowledge of the long-term frequency and intensity of drought events in an area is crucial since drought has adverse effects on natural ecosystems, food security, economy, society, and civilization. We developed a 405-year long (1611–2015C.E.) tree-ring chronology of *Pinus wallichiana* (Blue pine) from the Dolpo area of the trans–Himalayan region in Nepal to reconstruct drought variability in this remote region. Correlation analysis revealed significant positive relationships with February–August precipitation, but negative correlations with temperature. High positive correlations with the self-calibrated Palmer drought severity index (scPDSI) confirmed that moisture availability during the early growing season and full growing season is the primary limiting factor for Blue pine tree growth in the trans–Himalayan region. We used a linear regression model between our tree-ring record and regional climate data to reconstruct a 319-year long (1697–2015C.E.) February–August scPDSI series. This reconstruction accounts for 39.4% of the total variance in actual scPDSI over the calibration period (1957–2015C.E.). The reconstruction showed that the area was under slightly dry conditions for most of the reconstructed period, with below normal scPDSI values. An extreme drought was observed in the year 1707. Also, the years 1705, 1706, 1784, 1786, 1809, 1810, 1813, 1821, 1849, 1858, 1861, 1909, 1967, 2006, and 2009 experienced severe drought conditions. Consecutive years with moderate drought were 1702–1706, 1783–1789, 1796–1798, 1812–1814, 1816–1827, 1846–1848, 1856–1864, 1873–1877, 1879–1882, 1899–1901, 1908–1911, and 1967–1968. Three historic mega-drought events that occurred in Asia were also captured in our reconstruction: Strange Parallels drought (1756–1768), the East India drought (1790–1796), and the late Victorian Great Drought (1876–1878). Very few wet years (1776–1979, 1989, 1991, and 2003) were observed during the reconstruction period. Power spectrum analysis revealed drought variability at frequencies of 2.0–2.5, 3.0, 12.0, and 128 years, suggesting that drought in the region might be linked to broad-scale atmospheric-oceanic variabilities such as the El Niño-Southern Oscillation (ENSO) and the Atlantic Multidecadal Oscillation (AMO). The results not only improve our understanding on regional drought variability, but are also helpful to make decisions on adaptation measures for protecting the marginal communities of the trans–Himalayan region from the anticipated adverse impacts of future droughts.

1. Introduction

The Himalayan region is very vulnerable to the impacts of climate change and associated disasters induced primarily by rapidly increasing temperature and frequently observed extreme rainfall events (Xu et al., 2009; Shrestha et al., 2012; IPCC, 2014; DHM, 2015; Panday et al.,

* Corresponding author.
E-mail address: fanzexin@xtbg.org.cn (Z.-X. Fan).

https://doi.org/10.1016/j.palaeo.2018.10.026
Received 23 March 2018; Received in revised form 14 October 2018; Accepted 24 October 2018
Available online 30 October 2018
0031-0182/ © 2018 Elsevier B.V. All rights reserved.

2015; Dahal et al., 2016; Karki et al., 2017). Rapid climate change in the region has posed severe threats to the stability of ecosystems in high-mountain terrain. In Nepal Himalayas, extreme drought events, both in winter and summer seasons, have become more frequent and intense over the past three to four decades (Sigdel and Ikeda, 2010; Wang et al., 2013; Kharel–Kafle, 2014; Dahal et al., 2016), with adverse impacts on agriculture, forestry, water resources, and livelihoods (MOE, 2010).

Physiographical division of Nepal Himalaya includes: Terai, Siwalik, Mahabharat range, Midlands, Fore-Himalaya, Higher-Himalaya, and Inner- or Trans-Himalaya. The rate of climate change and its impacts is different across these regions. Across the Nepal Himalayas, there is a general east-west gradient towards drier conditions due to a declining influence of the Indian Summer Monsoon (ISM) (Kansakar et al., 2004; Zurick et al., 2005; DHM, 2015). In addition, the pronounced and complex topography plays an important role in modifying regional climate (Kansakar et al., 2004; Böhner et al., 2015). Because of the rain-shadow effect, the north-facing sides of the Himalayas as well as the inner or trans-Himalayan regions are characterized by much drier climatic conditions than the southern slope of the Himalayas (Kansakar et al., 2004; DHM, 2015). For example, mean annual precipitation in Dunai in the trans-Himalayan region, is about 350 mm while the country's average is about 1800 mm (DHM, 2015). As a consequence, the dominant forest types in the trans-Himalaya comprise drought-tolerant species such as junipers and pines in contrast to the lush conifer forests of fir, hemlock, and spruce in the southern slopes of the main Himalayan crest line (Miehe et al., 2015; Yadava et al., 2016).

Information of long-term hydro-climatic variability is crucial for evidence based decision-making, and formulation of appropriate adaptation policies and programs for improving climate resilience of the local population (IPCC, 2014). However, the available meteorological records of the Himalayan region are still too short for long-term trend analysis and for reliable estimations of future climate change (Shrestha et al., 1999, 2012; DHM, 2015). Natural archives such as tree rings, ice cores, and lake sediments can be used as climate proxies to extend climate records in the region (Bhattacharyya et al., 1992; Cook et al., 2003; Borgaonkar et al., 2010; Bhushan et al., 2018). Among the available proxies, tree rings are considered most suitable because of high dating accuracy, and annual to sub-annual resolution (Fritts, 1976). Tree rings in Nepal have been successfully used to reconstruct temperature (Cook et al., 2003; Sano et al., 2005; Thapa et al., 2015), drought (Sano et al., 2012; Panthi et al., 2017) and precipitation (Gaire et al., 2017). All these studies are primarily based on southern declivity sites of the Nepal Himalaya. Dendroclimatic studies focusing in the trans-Himalayan regions are crucial to improve the spatial coverage of regional paleoclimatology.

Knowledge of the frequency and intensity of the long-term trend of drought occurrence is essential, not only for the management of water, energy, and agro-forestry resources in the context of climate change, but also for protecting people's livelihoods (IPCC, 2014). There are several examples in history where droughts are hypothesized to be one of the major causes of societal changes, armed conflicts, and even societal collapses (e.g., Weiss and Bradley, 2001; Buckley et al., 2010; Pederson et al., 2014; Beach et al., 2016; Weiss, 2016; Yadava et al., 2016). The Dolpo in the trans-Himalayan region of Nepal is the home for many ethnic communities who are living in water stressed conditions. These communities depend on agriculture and forests of *P. wallichiana* for their livelihood in terms of fuel-wood and timber. These communities of the Dolpo region have experienced impacts of climate change (McChesney, 2015; Aryal et al., 2017). Therefore, with the projected rate of global climate change and its impacts on agriculture, forests, biodiversity, and water resources, the marginalized communities will be affected the most. In addition to knowing how *P. wallichiana* in the region has responded to climate change and how the species can cope with anticipated extreme climate in future, findings on the frequency and intensity of historic droughts events will be useful for protecting marginal communities and their culture/civilizations from future adverse impacts.

Pine trees are very sensitive to moisture, and are therefore extensively used as hydro-climate proxies at different spatio-temporal scales across the region (Li et al., 2006, 2007; Cook et al., 2010; Fang et al., 2010, 2012; Lu et al., 2013; Yadav, 2013). Blue pine (*Pinus wallichiana* A. B. Jackson) is an evergreen coniferous tree distributed across the Hindu-Kush, Karakoram, and Himalayas spanning from eastern Afghanistan to northern Pakistan, India and Nepal, to Yunnan in southwest China (Devkota, 2013). It is found growing at elevations of 1800–4300 m, and in some places, it reaches up to the treeline (Dubey et al., 2003; Shrestha et al., 2015). It grows well in temperate climates with dry winters and wet summers with mean annual rainfall of 250 to 2000 mm. It prefers well-drained soils, and can also grow on limestone if the soil above the rock is deep enough (Farjon, 2011). It also forms old-growth forests as the primary species or in mixed forests with *Betula utilis*, *Cedrus deodara*, *Picea smithiana*, and *Abies* spp. (Stainton, 1972). The species has been suggested to be suitable for reconstruction of hydro-climate (Bhattacharyya et al., 1992; Schmidt et al., 1999; Cook et al., 2003; Bräuning, 2004; Shah and Bhattacharyya, 2012) and regional glacier dynamics (Bhattacharyya and Yadav, 1996; Singh and Yadav, 2000). The *P. wallichiana* trees also tend to have a strong common signal compared to the other species and are potentially sensitive to drought in the Nepal Himalayas (Thapa et al., 2017). However, climate reconstructions based only on *P. wallichiana* tree-rings have not yet been attempted from the Nepal Himalaya region.

Previous dendroclimatic reconstructions from the Nepal Himalayas are still few in number (Cook et al., 2003; Sano et al., 2005, 2012; Thapa et al., 2015; Gaire et al., 2017; Panthi et al., 2017) and have limited scope for generalizations of the climatic trends over the entire central Himalaya (Nepal). Most tree-ring based climate reconstructions have been conducted in the southern declivity of the High Himalayas, and until now no dendroclimatic study has been carried out focusing mainly on the inner- and trans-Himalaya. Therefore, more studies are required covering the diverse hydro-climatic situations and heterogeneous topography of the region. It is essential to improve the spatial coverage of this regional climate proxy in the trans-Himalaya since it is under-represented in previous tree-ring samplings. Hence, this study is a new contribution for understanding the climate of the inner- and trans-Himalayan region. The major objectives of this study were i) to contribute a tree-ring chronology network for the inner- and trans-Himalaya and ii) to reconstruct the long-term drought history of the inner- and trans-Himalayan region.

2. Materials and methods

2.1. Study site and sample collection

The study was carried out in the Dolpo region that is protected under the Shey Phoksundo National Park (SPNP). The SPNP is a trans-Himalayan protected area that covers 3555 km^2 with an elevation spanning from 2130 to 6885 m asl (DNPWC, 2015). The park harbors the Shey Phoksundo Lake, the deepest lake of Nepal at 3612 m, which is also included in the Ramsar convention site (DNPWC, 2015). The forested area comprises only about 5% of the park that is mostly confined to south-facing slopes. The regional flora includes *Rhododendron* spp., *Caragana* spp., *Salix* spp., *Juniperus* spp., *Birch* spp., and occasionally *Abies* dominating the high forests of the Himalayas (DNPWC, 2015). For example, in the Suligad valley of the park, prominently occurring tree species are: *Abies spectabilis*, *Cedrus deodara*, *Picea smithiana*, *Pinus wallichiana*, *Populas* spp., *Rhododendron* spp., and *Tsuga dumosa* (DNPWC, 2015).

Field work and sample collection was carried out in April 2016. We collected core samples from the least anthropogenically-disturbed forest stand of *P. wallichiana*. The stand was located on a ridge of the mountain (29.168943° N, 82.945969° E) on the southeastern side of

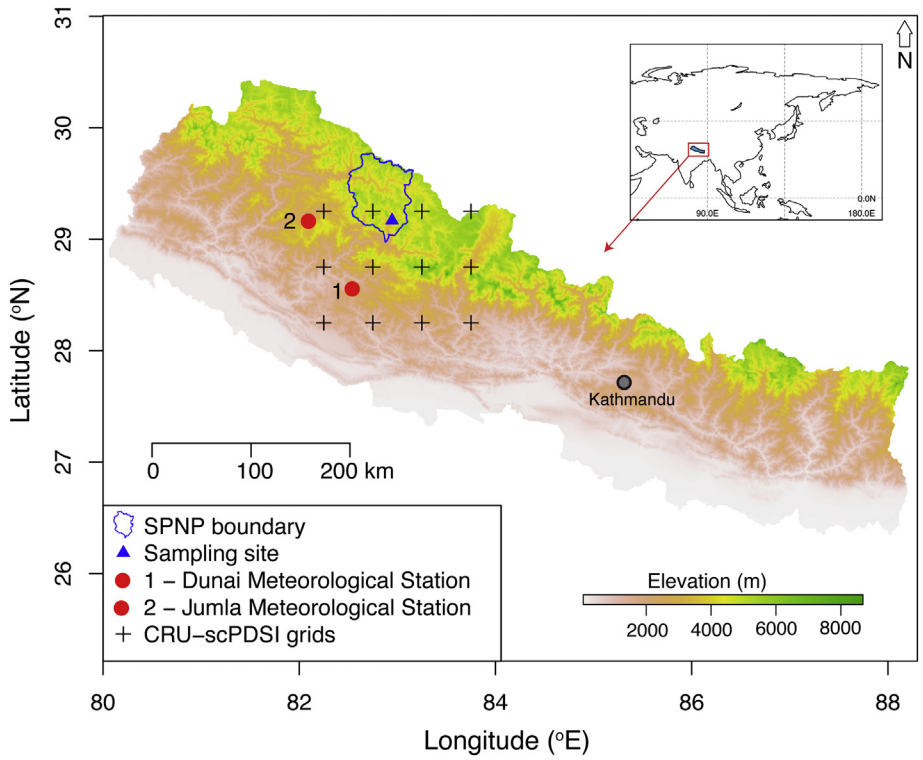

Fig. 1. Location map of the study area (SPNP - Shey Phoksundo National Park), sampling site, meteorological stations, and climate data grid points.

Shey Phoksundo Lake (Fig. 1). The slope of the sampling site ranged from 30 to 40°. The sampling site covers an elevation range from 3750 to 3950 m. Tree cores were collected using an increment borer (Haglof, Sweden) following the commonly used technique (Fritts, 1976; Cook and Kairiukstis, 1990; Speer, 2010). The cores were collected at breast height (1.3 m) and two cores per tree were collected where possible. A total of 52 cores were collected.

2.2. Tree-ring sample analysis and chronology development

The collected tree core samples were brought to the laboratory for preparation and measurement. The cores were mounted in wooden frames by using adhesive with the transverse surface of the core facing up. After air drying, cores were sanded and polished by a belt sander using successively finer grades of sand paper (120 to 600 grit) until optimal surface resolution allowed annual rings to be visible under the microscope. Each ring was counted under a stereo zoom microscope (Leica) and assigned a calendar year with the help of the known date of formation of the outer rings. The width of each ring was measured to the nearest 0.01 mm precision with the LINTAB™5 measuring system attached to a PC with the TSAP–Win software package (Rinn, 2003). All tree cores were crossdated by matching patterns of relatively wide and narrow rings to account for the possibility of ring-growth anomalies such as missing rings, false rings, or measurement error (Fritts, 1976). The pointer year technique was also used to identify narrow and wide pointer growth years. Each tree-ring width series was visually (using the math graphs) and statistically (using Gleichläufigkeit, t-values, and the crossdate index-CDI) crossdated using the software package TSAP–Win (Rinn, 2003). Accuracy of crossdating and measurement were further checked using the COFECHA program (Holmes, 1983; Grissino–Mayer, 2001). Two young (< 40 years) core samples with irregular growth patterns were discarded from final analysis and chronology.

Each tree-ring width series were standardized using negative exponential curve in signal-free standardization method (Melvin and Briffa, 2008; Briffa and Melvin, 2009). The standardization removes the growth trends related to tree age and geometry as well as tree-to-tree competition and stand dynamics while preserving variations that are likely related to climate (Cook, 1985; Cook and Kairiukstis, 1990). The signal-free method generates a series of detrending curves that are free of growth patterns common to all measurement series and preserves low to medium frequency signal in the final chronology (Melvin and Briffa, 2008). The standardization was carried out in computer program RCSSigFree (http://www.ldeo.columbia.edu/tree-ring-laboratory/resources/software). Individual detrended series were averaged using a bi-weight robust mean function (Cook, 1985; Cook and Kairiukstis, 1990) to produce the mean chronology. Various chronology statistics like mean sensitivity (MS), standard deviation (SD), expressed population signal (EPS), signal-to-noise ratio (SNR), running mean inter-series correlation coefficient (Rbar), variance explained by the first principal component (PC) were calculated to assess the dendroclimatic potential of the chronology (Fritts, 1976; Briffa, 1995; Speer, 2010).

2.3. Climate of the study area

The SPNP experiences a wide range of climatic conditions and lies in the transition zone from a monsoon dominated to an arid climate (DNPWC, 2015). Most parts of the SPNP lies in a rain shadow. The Dhaulagiri and Kanjiroba massifs form a large barrier that prevents most of the monsoonal rain from reaching the trans-Himalayan area. Winter is severe with frequent snowfall and temperature remaining below freezing above 3000 m while summer is warm. The nearest meteorological station is located at Dunai, which is about 60 km south-west from the tree-ring sampling site. Temperature and precipitation data are available for the period of 1989–2013 and 1984–2014, respectively. Another nearer station is Jumla, which is about 70 km west from the sampling site. Missing values in the data were filled with linear interpolation techniques. Most of the annual rainfall occurs during summer from July to September (Fig. 2A). The mean annual total precipitation at Dunai station (elevation 2058 m asl), Dolpo region is 347.6 mm (range: 13 to 741 mm). Over the observation period, the station experienced a decreasing trend in precipitation by 11.9 mm/yr

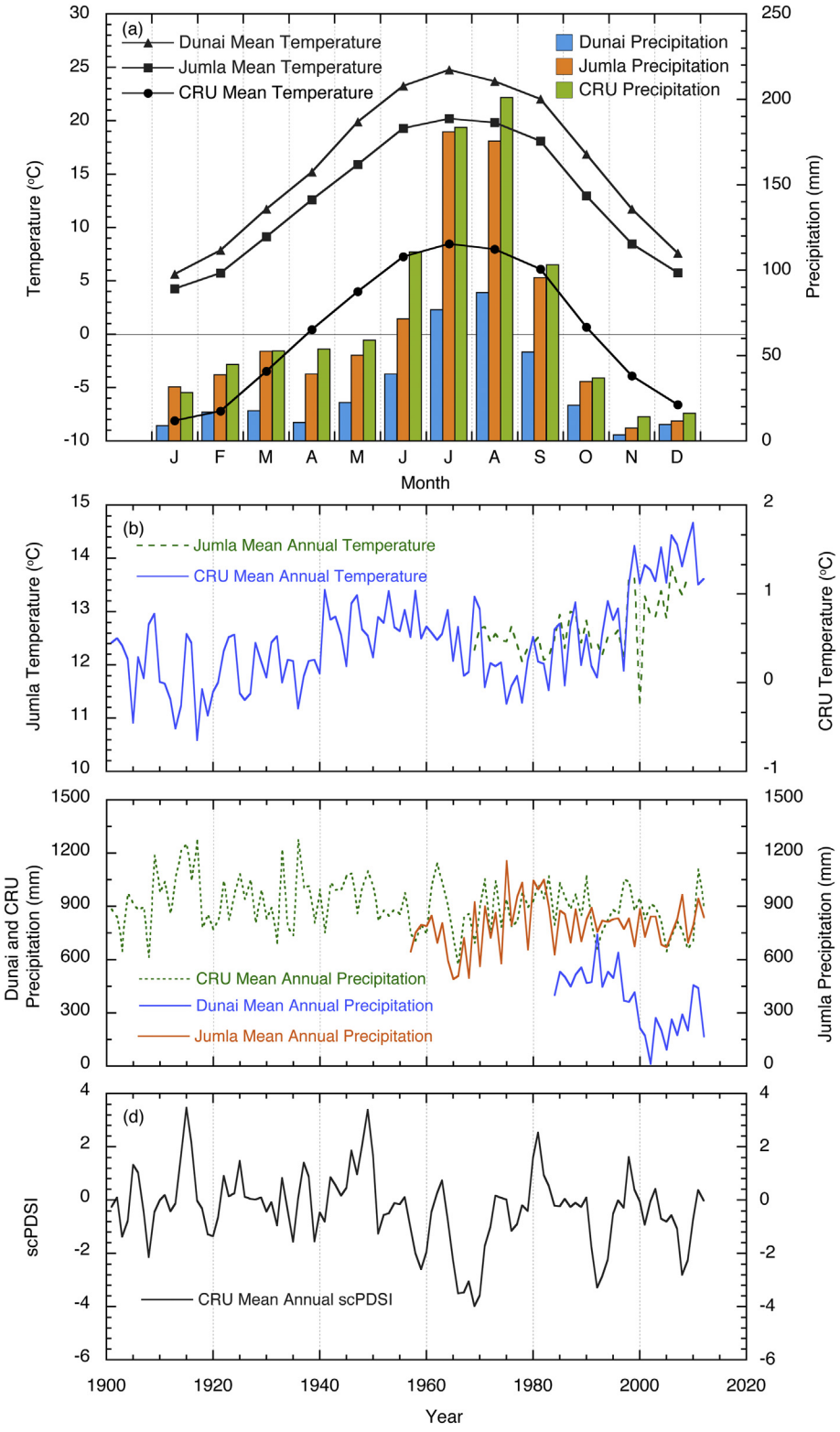

Fig. 2. Climograph for two meteorological stations (Dunai, Jumla) and averaged grid-point climate data (CRU, see method section for details) near the Shey Phoksundo National Park area in the central Himalaya (A); mean annual temperature of CRU data and Jumla station (B); Annual total precipitation of CRU data and at Dunai and Jumla stations (C); and annual trend of CRU's scPDSI averaged for 12 grid points covering the study region (D).

(Fig. 2B). The highest (34.4 °C) and lowest (−2.9 °C) monthly mean temperatures in Dunai are recorded in August and January, respectively. There is no significant trend in the mean annual temperature, but a decreasing trend in annual mean maximum temperature ($p < 0.05$), and an increasing trend in minimum temperature ($p > 0.5$) in recent years (graph not shown). The mean annual rainfall in Jumla station is 794 mm (SD = 140) which is higher than in Dunai. The mean annual temperature at Jumla has significantly increased by 0.02 °C/yr ($n = 44$, r = +0.54, $p < 0.01$) during 1969–2012 (Fig. 2C). Similarly, the annual total precipitation has also increased (Fig. 2D) by

1.76 mm/yr during 1957–2012, however this increase is statistically not significant ($n = 56$, $r = +0.21$, $p > 0.05$). The CRU (Climate Research Unit) regional grid data, with an average of 12 grid points also covering the park, show an increasing trend in average annual temperature (Fig. 2B) and slight decreasing trend in annual precipitation (Fig. 2C).

There are several indices to represent drought in an area. Among others, the Palmer's Drought Severity Index (PDSI; Palmer, 1965) and the Standardized Precipitation Index (SPI; Agnew, 2000) are commonly used drought indices. In this study, we used the improved form of PDSI known as self-calibrating Palmer Drought Severity Index (scPDSI) (van der Schrier et al., 2013), which is based on a supply-and-demand model of soil moisture and is an effective indicator in determining long-term droughts of several months to years. In our study area, scPDSI data shows a trend towards increasing drought conditions (Fig. 2D).

2.4. Response of tree growth to climate

Long instrumental climatic records are a pre-requisite to examine the response of tree growth to climate. However, due to the lack of availability of long instrumental climate records close to the tree-ring sampling site, we used gridded climate records. We obtained 0.5° CRU TS 4.00 records for mean temperature (here after CRU-T), precipitation (hear after CRU-P), and CRU scPDSI (here after drought). Initially, 30 series of 0.5° gridded CRU-T, CRU-P and drought were selected covering the entire western Himalayan region. Point-by-point correlations between our tree-ring chronology and climate variables were calculated for a 14-month dendroclimatic window starting from September prior to the growth year and ending in the following October. After preliminary examination, significant seasonal climatic variables were selected, and the model of point-by-point correlation was calculated again for 12 regional grids of CRU-T, CRU-P, and drought. The most promising candidate variables explaining the physiological mechanism of growth control of *P. wallichiana* was selected further for reconstruction. The calibration period selected for the present study is 1957–2015C.E.

2.5. Drought reconstruction methodology

A simple linear regression model was established between averaged spring–summer (February–August) scPDSI for 12 grid points and the tree-ring chronology to reconstruct drought for the central trans-Himalaya. The time stability of the model was tested by using calibration and verification methods (Michaelsen, 1987; Snee, 1997; Meko and Graybill, 1995). Due to the relatively short calibration period available for the split-half validation, we used the 'leave-one-out' cross-validation approach (Michaelsen, 1987). Estimated and actual drought data were subjected to various calibration and verification statistics, such as coefficient of determination (R^2), F statistics, and reduction of error (RE). Any positive value of RE and lowest root mean square of error (RMSE) in the verification are taken as a basis for validity and reliability of the regression model (Cook and Kairiukstis, 1990). In addition, the Durbin Watson (DW) statistics in the regression model was calculated to test the autocorrelation of residuals. Once the model was judged effective and stable, it was applied to reconstruct drought of the spring–summer season (February–August). The reconstruction period was truncated at the point in which EPS decreased below the commonly recommended threshold value of 0.85 (Wigley et al., 1984). Extrapolations in the reconstruction, or reconstructed values for years in which the predictors were outside the multivariate space in the calibration period were identified using the ellipsoid method (Weisberg, 1985). Based on scPDSI values, drought can be categorized as incipient, slight/mild, moderate, severe, or extreme (van der Schrier et al., 2013). The scPDSI uses a "0" as normal, and drought is indicated by negative numbers; for example, −0.5 to −1.0 is incipient dry, −1 to −2 is mild/slight drought, −2 to −3 is moderate drought, −3 to −4 is severe drought, and < −4 is extreme drought. Positive values indicate wet periods of the same category (van der Schrier et al., 2013), respectively. The reconstruction was further analyzed for its time-series variability. We also compared the extreme-dry and extreme-wet periods (expressed as mean ± 1 sigma) in our drought reconstruction with those in other independent tree-ring based drought and precipitation reconstructions from the Nepal Himalaya and adjoining regions to analyze spatio-temporal variations of drought.

2.6. Spatial correlation and teleconnections

Spatial correlation analysis was performed to investigate the spatial representation of our reconstructed scPDSI. Spatial correlations were performed using the KNMI Climate Explorer (Trouet and Oldenborgh, 2013; http://climexp.knmi.nl/) and correlation coefficients were represented in the field ($p < 0.05$). Power spectral analysis of our spring–summer drought variation was performed using the Multiple-Taper Method (MTM) (Mann and Lees, 1996). Spatial correlation analysis was computed between reconstructed scPDSI with Hadley Centre Sea Ice and Sea Surface Temperature (HAD1-SSTs) to evaluate the coherency and teleconnections of spring–summer drought with global climate drivers.

3. Results

3.1. Ring-width chronology

Based on the ring-width analysis of 50 tree core samples, we developed a 405-year long ring-width chronology of *P. wallichiana* extending from 1611 to 2015C.E. (Fig. 3). The average radial growth rate of *P. wallichiana* was 1.35 mm/yr (SD = 0.89). The chronology revealed distinct high and low growth periods during the last four centuries. The radial growth of *P. wallichiana* increased continuously since the early 19th century until the end of the 20th century. The narrowest rings were observed in the years 1705, 1706, 1810, 1909, 1967, and 2009, while widest rings were observed in the years 1669, 1776, 1928, and 1991. The chronology statistics calculated for the whole chronology time span and for the period covered by most of tree-ring series showed a high dendroclimatic potential of the species, with a moderate mean sensitivity (0.156), standard deviation (0.229), reliable EPS (0.955), high SNR (21.23), and moderately high variance explained in the first PC (39%). The inter-series correlation was also high (Rbar = 0.653).

3.2. Growth climate response

Spatial correlation between the tree-ring chronology of *P. wallichiana* and gridded regional climate records revealed that our chronology captured the climatic signal from a large part of the central Himalaya and is therefore representative for the region (Fig. 4A–C). Simple correlation analysis between the tree-ring chronology of *P. wallichiana* and CRU gridded temperature showed that tree growth is negatively correlated with temperatures in most of the months of the current growth year (Fig. 4D). The relationship is strong and significant ($p < 0.05$) with the temperatures in previous year September, January to June, and August of the current year, and the whole spring–summer season (February–August) of the current growth year (Fig. 4D). At the same time, there was a positive correlation between tree growth and precipitation (rainfall) for most of the months of the current growth year (Fig. 4E). The correlation between radial tree growth and rainfall in November–December of the previous year, and current year February, April, June, July, and August was significantly positive ($p < 0.05$) (Fig. 4E). There was a significant positive ($p < 0.05$) correlation between the tree-ring chronology of *P. wallichiana* and scPDSI from the previous year September to the current growth year September, with the strongest correlations during the spring and summer months ($r > +0.50$, $p < 0.05$) (Fig. 4F).

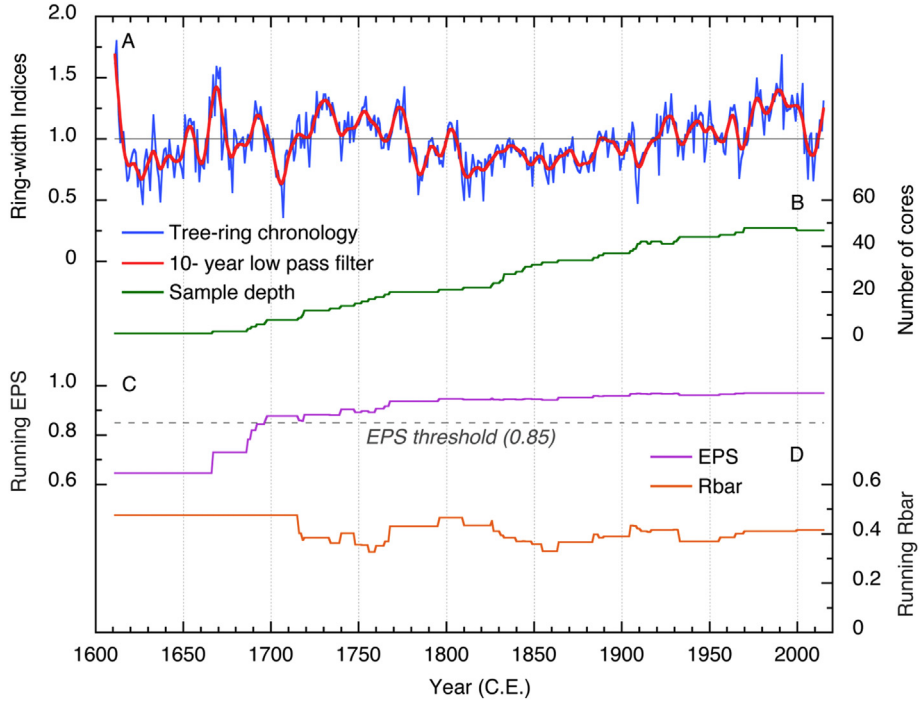

Fig. 3. Tree-ring chronology (with 10-year low pass filter) of *Pinus wallichiana* from the Shey Phoksundo National Park, Nepal Himalaya (A); number of sampled cores included in the tree-ring chronology (B); running inter-series correlation (Rbar) and expressed population signal (EPS) statistics (C and D).

3.3. Drought history reconstruction for the trans-Himalaya

Based on the response of *P. wallichiana* tree growth to various climatic variables, spring–summer (February to August) drought became the best candidate for reconstruction. The regression model explained 39.4% of the actual variance in the climate data, and was subjected to the F-test of significance using the entire climate records available i.e., 1957–2015C.E. The regression model showed a positive value of RE (0.35), indicating robustness of the model (Fritts, 1976) (Fig. 5A). The RMSE value is considerably smaller (1.31) than the standard deviation (1.64) of the actual scPDSI over the calibration period. Regression residuals are normally distributed, and the lack of first-order autocorrelation in residuals was supported by the Durbin–Watson statistic test.

Using the ring-width chronology of *P. wallichiana* from the Shey Phoksundo Lake area of Dolpo region of Nepal, a 319-year spring–-summer drought reconstruction was developed for the period 1697 to 2015C.E. (Fig. 5B). The average scPDSI was −1.412, indicating mild dry conditions over the reconstruction period. The reconstructed scPDSI showed many episodes with prolonged drought during the 19th and 20th century. The years 1705, 1706, 1784, 1786, 1809, 1810, 1813, 1821, 1849, 1858, 1861, 1909, 1967, 2006, and 2009 experienced severe drought conditions. Consecutive years with moderate drought (1702–1706, 1783–1789, 1796–1798, 1812–1814, 1816–1827, 1846–1848, 1856–1864, 1873–1877, 1879–1882, 1899–1901, 1908–1911 and 1967–1968), some of which overlapped with severe drought years (1810, 1813, 1821, 1909), and extreme drought (1707) were also recorded (Fig. 5B). Another interesting finding is the recurrence of extreme droughts in centennial time periods (1707, 1809, 1909, and 2009). There were many mild drought years. We also observed few incipient (1776, 1979, 1989, and 2003) and very few moderately wet (1977 and 1991) spring–summer years during the recent three centuries.

3.4. Spatial representation and teleconnections

The dry and wet periods observed in the present drought reconstructions were also recorded in other reconstructions (Fig. 6; Supplementary Fig. S1 and S2). The spectral and wavelet analyses of the drought record revealed that droughts in the central trans-Himalayas display both high (2–3 yrs. and 12 yrs.) and low (128 yrs.) frequency cycles (Fig. 7). We found strong positive correlations between the reconstructed droughts and SSTs of the Indian Ocean and the Equatorial region of the Pacific Ocean, and negative correlations with SSTs in the North Atlantic Ocean (Fig. 8). This indicates teleconnections between droughts in our study area with the broader scale circulation systems and climate-modes.

4. Discussion

We developed a 405-year long ring-width chronology of *P. wallichiana* extending from 1611 to 2015C.E. The chronology statistics (MS, SD, EPS, SNR and Rbar) indicated a high dendroclimatic potential of this pine species (Fritts, 1976). The EPS was above the threshold limit of 0.85 (Wigley et al., 1984) since 1697C.E, which suggests that the chronology is less reliable before 1697C.E. due to poor sample replication in the earlier part of the chronology. The chronology characteristics (MS, SD, EPS, SNR, and Rbar) are within the range of values obtained for the same and other pine species in the Himalayas (Bhattacharyya et al., 1992; Cook et al., 2003; Bräuning, 2004; Shah and Bhattacharyya, 2012; Yadav, 2013). The most narrow pointer years observed in present study (1705, 1706, 1810, 1909, 1967, and 2009 CE) were also observed in other chronologies from the western (Sano et al., 2005; Thapa et al., 2015, 2017; Gaire et al., 2017; Panthi et al., 2017) and eastern Nepal Himalaya (Dawadi et al., 2013; Liang et al., 2014; Kharal et al., 2017). The growth of *P. wallichiana* consistently increased from the mid-19th century to the late-20th century. The observed enhanced growth of *P. wallichiana* during the 20th century is consistent with other studies from the Himalaya and adjacent regions. For example, Borgaonkar et al. (2009, 2011) reported increased growth of *P. wallichiana*, *Cedrus deodara*, and *Picea smithiana* from high-altitude forests in Kinnuar and Gangotri region, India; Gou et al. (2007) and Liang et al. (2009) made similar observations in other conifer species on the Tibetan plateau and adjacent mountain regions.

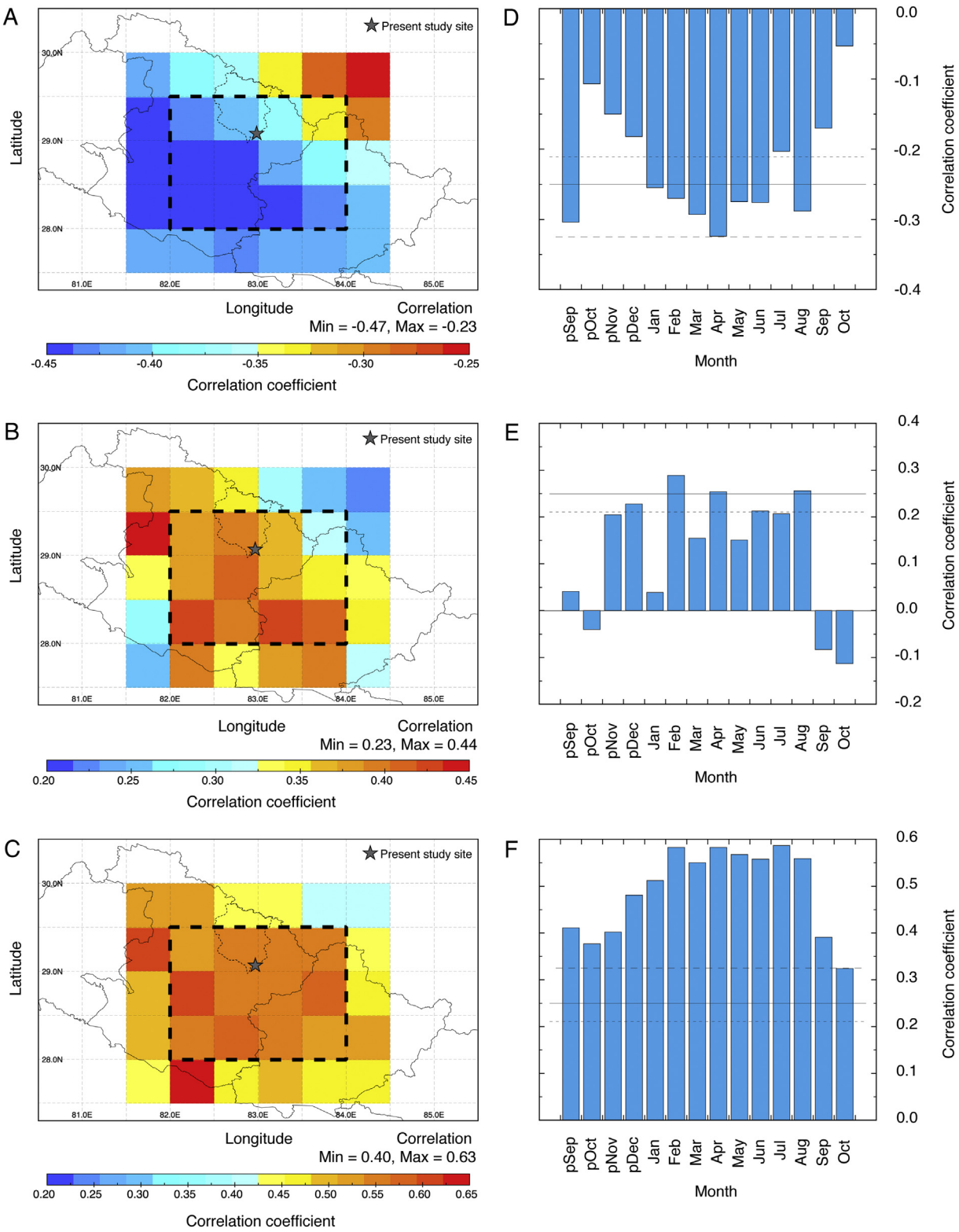

Fig. 4. Spatial correlations between a tree-ring chronology of *Pinus wallichiana* and gridded climate records: (A) temperature, (B) precipitation and (C) scPDSI for 30 grid points; and correlations between tree-ring chronology and averaged climate records of 12 grid points (thick dotted square boundary in left panels) and (D) temperature, (E) precipitation and (F) scPDSI. Horizontal dotted line, straight line and dashed line represent 90%, 95%, and 99% confidence limits for a two–tailed test, respectively.

Correlation analysis between the radial growth of *P. wallichiana* and climatic parameters showed seasonal responses (Fig. 4). The negative response with temperature and positive response with precipitation and scPDSI indicates that moisture is predominant limiting factor for radial growth of *P. wallichiana*. Our study site in Dolpo lies in an arid region of the inner- and trans-Himalaya with < 300 mm of annual precipitation. In such environments, high temperatures without adequate moisture supply increase the evapotranspiration demand that ultimately limits

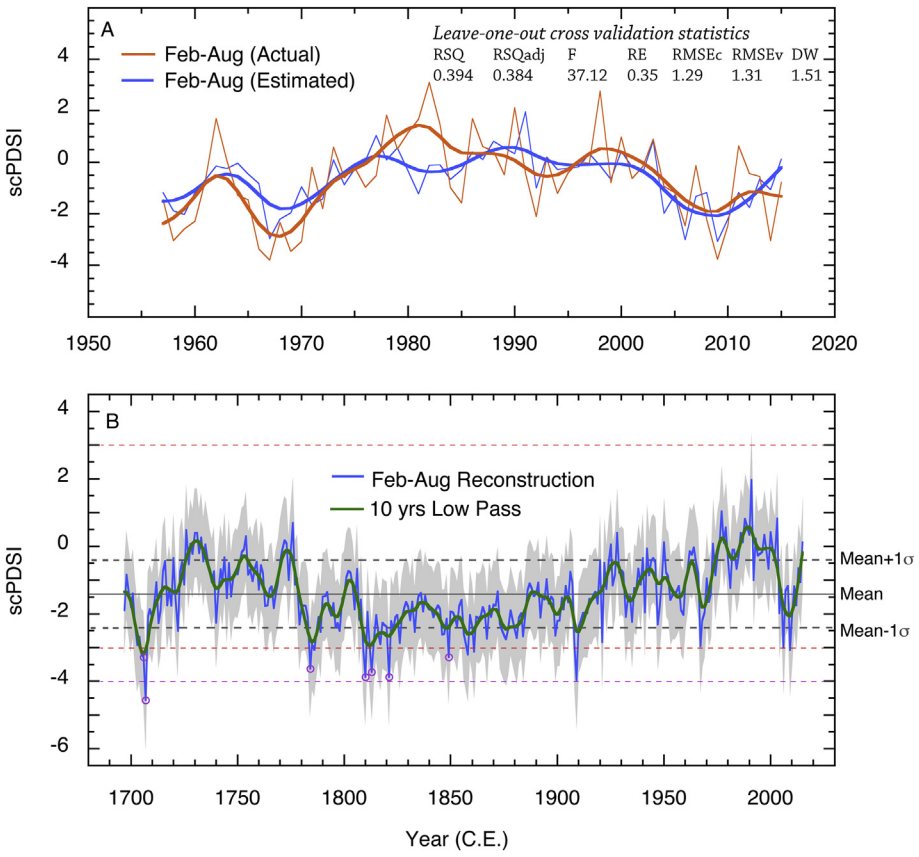

Fig. 5. (A) Actual and estimated February–August self-calibrated Palmer drought severity index (scPDSI) for 1957–2015C.E. (B) Reconstructed February–August scPDSI for 1697–2015C.E. along with 10 years low pass filter, mean of the long term reconstruction, upper and lower threshold based on mean ± 1 standard deviation. The red dotted lines are threshold lines for severe drought or wet condition; and purple dotted lines are threshold line of the extreme drought or wet condition. Purple circles mark the 7 reconstruction years classified as extrapolations identified using ellipsoid method (Weisberg, 1985). (For interpretation of the references to color in this figure legend, the reader is referred to the web version of this article.)

plant growth (Fritts, 1976; Cook et al., 2003; Sano et al., 2005; Kharal et al., 2017). In contrast, high precipitation throughout the year would be beneficial for growth (Fritts, 1976). Therefore, in dry and semi-arid inner valleys in the Himalaya, moist and cool years with below average temperature during the growing season would be beneficial for the growth of many conifer species including *P. wallichiana* (Cook et al., 2003; Bräuning, 2004; Shah and Bhattacharyya, 2012; Gaire et al., 2014; Kharal et al., 2017). The progression in radial growth during the 19th and 20th century in the region could be favored by cool/mild and moist summers and warm winters, as revealed by dendroclimatic reconstructions (Cook et al., 2003; Sano et al., 2005; Gaire et al., 2017). There were several short to medium (few years to some decades) periods with high precipitation in western Nepal during the past 170 years (Gaire et al., 2017). The growth enhancement in recent years might be, to some extent, caused by the observed decreasing trend in the annual maximum temperature in the region.

The growth-climate response observed in Dolpo region is similar to the response of several other pines and conifer species from drier regions in the Nepal Himalaya (Cook et al., 2003; Gaire et al., 2017; Kharal et al., 2017; Panthi et al., 2017), the western Indian Himalaya (Yadav, 2009, 2013; Ram, 2012), the Tibetan Plateau and other mountainous regions in China (Bräuning, 2001; Fang et al., 2010, 2012; Lu et al., 2013). Higher mean, maximum, and minimum temperatures during the summer season were not found to be conducive for the growth of trees in many dry sites in the Himalayas (Ram, 2012). A previous study from the upper Dolpa region (Bräuning, 2004) also found a significant positive relationship between the growth of *P. wallichiana* and precipitation during April to September of the current year. In the north-east Indian Himalaya, *P. wallichiana* exhibited a significant positive relationship with precipitation during current year January and June (Shah and Bhattacharyya, 2012). It was only minimum temperatures of the previous year that showed significant negative relationships with the growth of *P. wallichiana* in north-east India (Shah and Bhattacharyya, 2012).

A significant positive ($p < 0.05$) relationship between *P. wallichiana* growth and scPDSI in the concurrent year, with a stronger positive relationship during spring and summer months was observed (Fig. 4F). This indicates that soil moisture during spring–summer season plays a significant role for the growth of this conifer species. Temperature-induced drought may be common in severely dry regions or locations with shallow soil, where the potential evaporation is considerably higher than the actual evaporation (Fang et al., 2012). For such dry regions, the drought-growth correlations are expected to be high (Fang et al., 2012). We found higher correlations between tree growth and scPDSI compared to that between the tree growth and temperature or precipitation. Similar drought-stressed growth signals were also observed in dry mountain valleys in the Himalaya and other marginal regions of monsoon Asia (Cook et al., 2003; Fang et al., 2010, 2012; Singh et al., 2009; Yadav, 2009; Shah and Bhattacharyya, 2012; Lu et al., 2013). A positive relation between growth and PDSI is shared among many conifers, including *Abies pindrow*, *Abies spectabilis*, *Picea smithiana*, *Cedrus deodara*, and pine species (*P. gerardiana*, *P. wallichiana*, *P. tabulaeformis*, and *P. armandi*) in the Himalayas and adjacent regions (Ram, 2012; Sano et al., 2012; Yadav, 2013; Fang et al., 2012; Lu et al., 2013; Panthi et al., 2017).

We reconstructed drought for the past 319 years (1697 to 2015C.E.) based on the well-replicated part of a *P. wallichiana* ring-width chronology. The reconstructed scPDSI explained 39.4% of the variability in observed drought in the region, which is comparable to the explained climatic variance in other dendroclimatic reconstructions from the Himalayas (Ram, 2012; Sano et al., 2012; Yadav, 2013; Yadava et al., 2016; Gaire et al., 2017; Panthi et al., 2017) and adjacent regions in China (Li et al., 2006; Fan et al., 2008; Fang et al., 2010, 2012; Song and Liu, 2011; Kang et al., 2013; Lu et al., 2013; Sun and Liu, 2013; Chen et al., 2014; Cai et al., 2015). On the basis of scPDSI values, van der Schrier et al. (2013) classified drought into incipient, slight/mild,

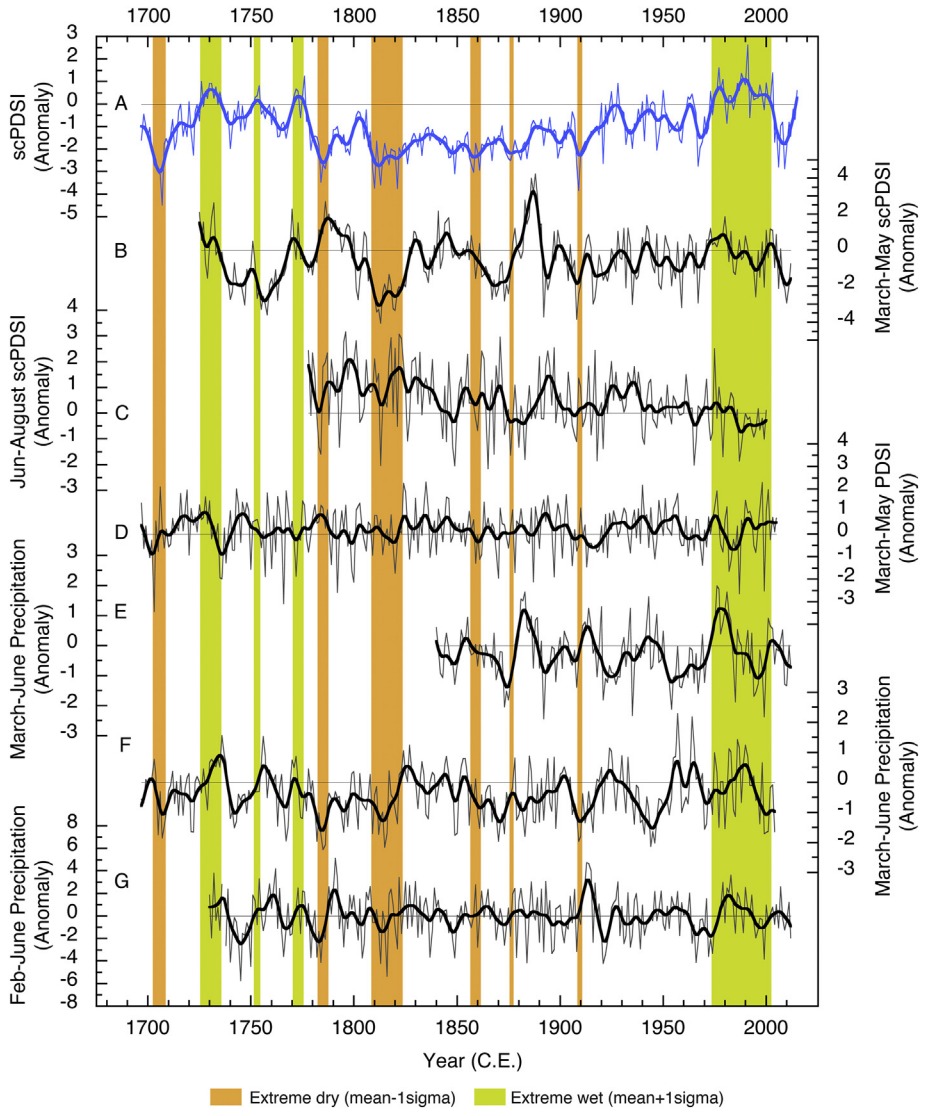

Fig. 6. Comparison of (A) reconstructed February–August scPDSI (this study) with (B) March–May scPDSI from western Nepal Himalaya (Panthi et al., 2017); (C) June–August scPDSI in north-western part of Nepal Himalaya (Sano et al., 2012); (D) March–May PDSI reconstruction in the central Hengduan Mountains, southwestern China (Fan et al., 2008); (E) March–June precipitation in Rara area, western Nepal Himalaya (Gaire et al., 2017); (F) March–July precipitation western, Indian Himalaya (Singh et al., 2009); and (G) February–June precipitation in Kumaon Hiamalaya, India (Yadav et al., 2014).

moderate, severe, and extreme categories. Over the reconstruction period, we observed droughts of different intensities at different time scales. The mean value of spring–summer scPDSI reconstruction is −1.412, which indicates overall mild drought conditions throughout the reconstruction period (Palmer, 1965; Alley, 1984; van der Schrier et al., 2013). However, there were few extreme and very few severe drought years with scPDSI value less than −3.0. One extremely dry (scPDSI ≤ −4.0), 14 severely dry (−4.0 < scPDSI ≤ −3.0) and 75 moderately dry (−3.0 < scPDSI ≤ −2.0) years occurred in our scPDSI reconstruction either in a single year or a series of consecutive years. One individual extreme drought year (1707C.E.) in the scPDSI reconstruction valued lower than −4.0. The periods 1699–1714, 1779–1800, and 1807–1827 experienced continuous droughts of different intensity. Severe droughts repeatedly occurred in centennial periodicity in the years 1707, 1809, 1909, and 2009.

Both observations (Sigdel and Ikeda, 2010; Wang et al., 2013; Kharel–Kafle, 2014) and tree-ring width based reconstructions (Sano et al., 2012; Panthi et al., 2017) have shown increasing numbers of drought years in western Nepal. Sigdel and Ikeda (2010) identified 1974, 1977, 1985, 1993, 1999, and 2001 as winter drought years, while 1977, 1982, 1991, and 1992 were summer drought years based on the Standardized Precipitation Index (SPI) of all Nepal precipitation data from 1973 to 2003C.E. Drought has not occurred synchronously across the Nepal Himalaya during the observation period. Another drought study conducted south-west of our study site using SPI data from 1982 to 2012 documented 1984, 1987, 1999, 2004, 2005, and 2009 as drought years for the Jumla region, and 1993 and 2006 for Musikot region (Kharel–Kafle, 2014). Some of these drought years are also documented in our present reconstruction. A recent tree-ring width based spring (March–May) PDSI reconstruction from western Nepal reported severe and extreme droughts in 1747, 1755, 1757–1758, 1763, 1811–1813, 1819–1820, 1873, 1892, 1908, 1916, 1935, 1959, 1967, and 2010 (Panthi et al., 2017). In the current reconstruction, only a few incipient (1776, 1979, 1989, 2003) and very few moderate (1977 and 1991) wet years were found. However, the Panthi et al. (2017) reconstruction found two very wet springs and five moderately wet springs during the past three centuries in the Jumla region. Some discrepancies in occurrences of drought years and their intensities of drought with other reconstructions in Nepal might be due to different target seasons and geography.

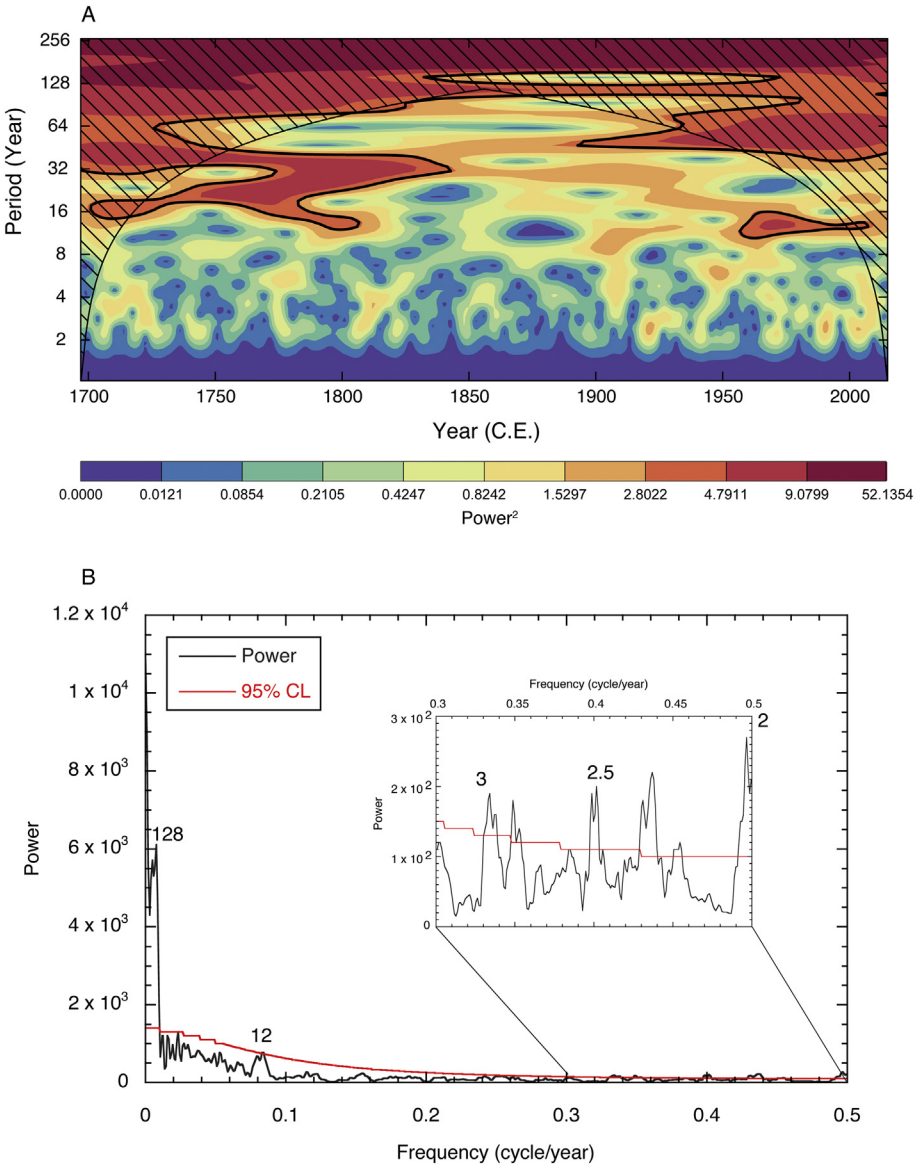

Fig. 7. Wavelet and Power spectral analysis for the reconstructed February–August scPDSI (1697–2015C.E.) in the central Himalaya. (A) Morlet global wavelet spectrum at 95% level of confidence (black lines/contours) based on red-noise background. The cross-hatched region of the cone depicts the spectrum with higher edge effects and (B) Power spectrum (black line) with red line representing 95% significance level. (For interpretation of the references to color in this figure legend, the reader is referred to the web version of this article.)

We also compared our drought reconstruction with tree-ring based drought or precipitation reconstructions from the Himalayas, adjacent regions in China, and broader Asia to test for coherency in long-term drought occurrence in the region (Fig. 6). Drought conditions could be local, regional, or global, and could be seasonal or annual and driven by temperature, rainfall, or both. In our reconstruction, there are several drought episodes that matched with other reconstructions. However, not all reconstructions matched perfectly, which might be due to differences in reconstructed indices of drought, seasons or location of the study. The trends observed in our reconstruction comply with the scPDSI reconstruction in western Nepal (Panthi et al., 2017). Aridity index reconstruction based on a tree-ring oxygen stable isotope chronology from the north-west corner of Nepal showed an increasing summer season aridity over the past two centuries (Sano et al., 2012), which matched with long-term drought during the 19th and 20th centuries in the current reconstruction. Spatial correlations (Supplementary Fig. S1 and S2) revealed that observed and reconstructed scPDSI correlated positively with the Monsoon Asia Drought Atlas (MADA) (Cook et al., 2010) and Dai PDSI (Dai et al., 2004) mainly in the central Himalayas. Our reconstruction captured three of the four mega-droughts captured in the MADA (Cook et al., 2010). The Strange Parallels drought (1756 to 1768), the East India drought (1790 to 1796), and the late Victorian Great Drought (1876 to 1878) (Cook et al., 2010; Kang et al., 2013) were also captured in the current reconstruction. In addition to these, we also observed extreme droughts in 1908–1911. Extreme dry periods during early 1700s, 1780s, 1810–20s, and 1860s were also captured in drought and precipitation reconstructions from the western Himalaya of India (Singh et al., 2009; Ram, 2012; Yadav, 2013; Yadav et al., 2014). In general, our reconstruction did not match perfectly with drought reconstructions from the Tibetan plateau and other areas of China (Li et al., 2006; Fan et al., 2008; Fang et al., 2010, 2012; Song and Liu, 2011; Kang et al., 2013; Lu et al., 2013; Peng and Liu, 2013; Sun and Liu, 2013; Chen et al., 2014). This discrepancy might be caused by the difference in precipitation regime between the Himalayas and China. However, some extreme drought events, for example in the early-18th century, mid-19th

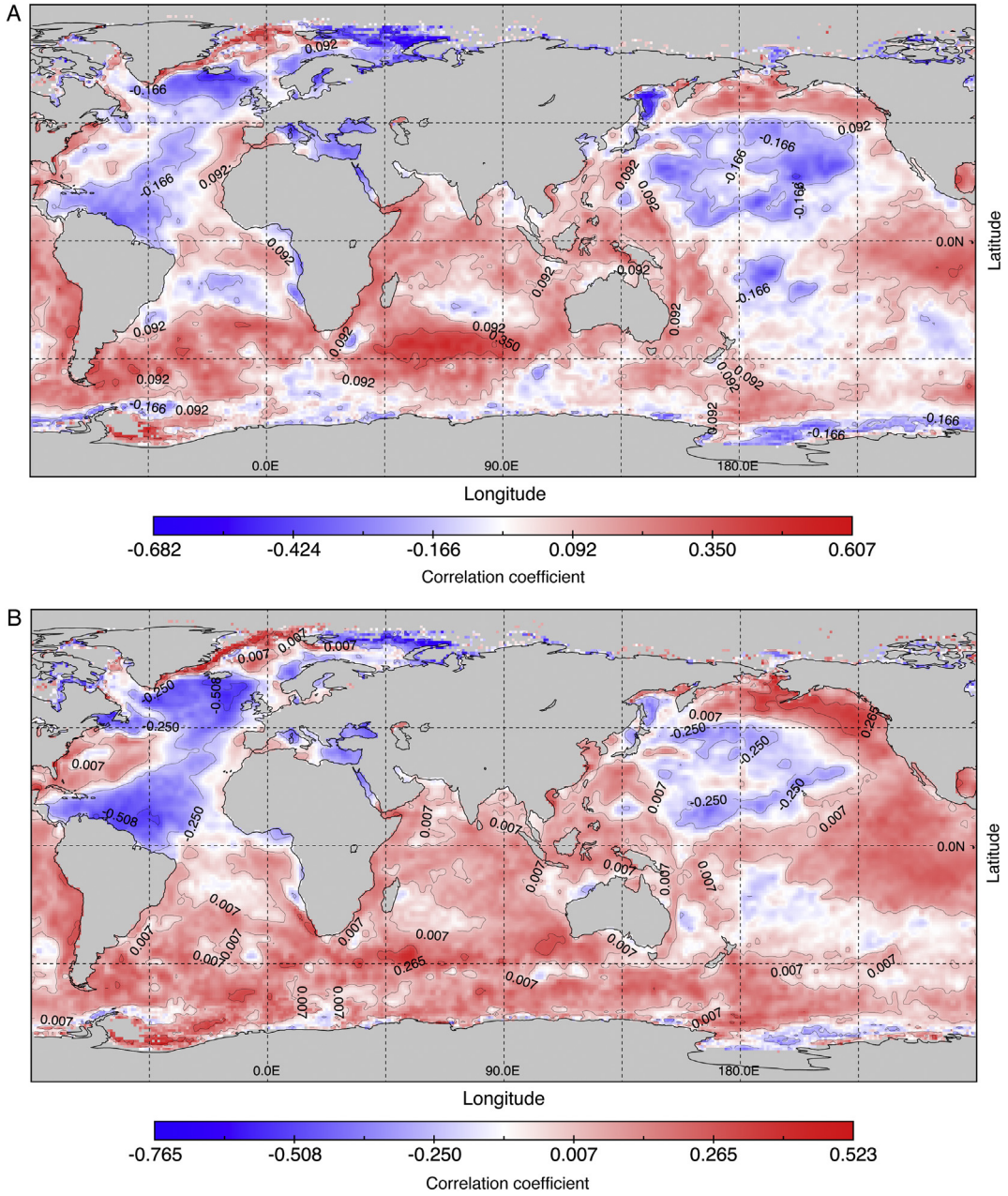

Fig. 8. Spatial correlations between actual (A) and reconstructed (B) spring–summer scPDSI with Had1SST1 for 1957 to 2014C.E.

century, and early-20th century were also captured in Chinese reconstructions (Fan et al., 2008; Kang et al., 2013; Sun and Liu, 2013). Fang et al. (2012) found extremely dry epochs during 1723–1727 and 1928–1932 in the Kongtong Mountain area in a tree-ring based May–-July PDSI reconstruction. The extreme drought events in 1877–1878 reconstructed by Kang et al. (2013) in the southeast Qilian Mountains, and droughts during 1700s and 1860s in the Hengduan Mountains in southwestern China (Fan et al., 2008) are also captured in the present reconstruction. Co-occurrences of several drought events across the region indicate a wider distribution of drought conditions during those periods.

Drought in a region can be influenced by local, regional, or global scale factors (Borgaonkar et al., 2010; Kang et al., 2013; Peng and Liu, 2013; Wang et al., 2013; Cai et al., 2015; Panthi et al., 2017). The Indian Summer Monsoon brings most of the precipitation to the Himalayan region, and its failure can cause drought. In addition to this, spring-summer drought variations over the western and central Himalayas are associated with large-scale ocean–atmospheric circulations (Yadav, 2013; Panthi et al., 2017). Wavelet and MTM spectral analysis revealed that drought in the region has both low and high frequency cycles, i.e. periodicities of 128, 12, and 2 to 3 years (Fig. 7), indicating that the spring–summer drought variability in the trans-Himalayan part of the central Himalaya might have remote connections with different circulation systems and climate-modes. The significant centennial-scale cycle (128 years) in the reconstruction is consistent with other drought reconstructions from the Tibetan Plateau (Fang et al., 2010; Peng and Liu, 2013; Wang et al., 2008). The high frequency cycles (2.0–3.0 years) in the present drought reconstruction fall in range of the ENSO (El-Nino Southern Oscillation) (Webster and Yang, 1992) and IOD (Indian Ocean Dipole Mode) (Saji and Yamagata, 2003). El Niño events could cause extensive droughts in the Asian monsoon region (Dai and Wigley, 2000). Influence of ENSO on droughts in the Himalaya has also been reported by several other studies (Singh et al., 2009; Sano et al., 2012; Gaire et al., 2017; Panthi et al., 2017). The

IOD's influence has also been reported from the Tibetan Plateau (Peng and Liu, 2013).

Further, spatial correlations between our reconstructed drought and SSTs in the Indian Ocean, Pacific Ocean, and the Atlantic Ocean suggest that in addition to variations in Indian Summer Monsoon and ENSO, the NAO (North Atlantic Oscillation) and AMO (Atlantic Multidecadal Oscillation) might be attributed to drought events in the trans-Himalaya. There was a significant positive correlation between the reconstructed spring-summer scPDSI with winter to early spring season HAD1-SST of the Indian Ocean and the equatorial Pacific Ocean, but a negative correlation with SST in the North Atlantic Ocean (Fig. 8). Warm (cool) SSTs over the North Atlantic Ocean are associated with dry (wet) spring–summer in the central Himalaya as also revealed by other studies (Panthi et al., 2017).

Droughts have been suggested to be one of the major causes of societal changes and collapses of several civilizations globally in the past (Weiss and Bradley, 2001; Pederson et al., 2014; Beach et al., 2016; Weiss, 2016). An assessment of the recent displacement of human settlements in the Mustang district, an adjacent district to our present study area, concluded that drought induced water scarcity was the main cause of displacement (Shrestha and Prasain, 2016). Our present study showed an increasing intensity and frequency of spring–summer drought over the past three centuries in the Dolpo region of the trans-Himalaya. Though there is a lack of written documentation on the historic drought events, peoples of the Dolpo region have been perceiving changes in the climatic variables, and experiencing impacts of climate change in their local environments and livelihoods (McChesney, 2015; Aryal et al., 2017). Knowledge generated from the present study about long-term drought history will be very useful, not only for raising awareness among local communities, but also to plan necessary adaptation measures by concerned authorities (i.e. local to national governments) and stakeholders in order to protect their livelihood and civilizations from anticipated adverse impacts of droughts.

5. Conclusions

A 405-year long ring-width chronology of *Pinus wallichiana* (Blue pine) was developed from the Dolpo area in the trans-Himalaya region of Nepal. Radial growth of *P. wallichiana* is limited mainly by moisture stress during the spring–summer season. The drought (scPDSI) reconstruction has identified several short to prolonged drought periods in the trans-Himalaya of Nepal during the past 319 years (1697–2015C.E.). Prolonged drought events were observed in 19th and 20th century. The reconstructed drought has variabilities at frequencies similar to those of broader scale climate-modes such as ENSO and AMO. Further, drought in Dolpo region is also significantly correlated with SSTs in the Indian Ocean and the Atlantic Ocean, which suggests that climate in this part of the trans-Himalaya might have remote connections with broad-scale atmospheric circulations. Further palaeoclimatic records in the trans-Himalaya would help strengthen the conclusion about such remote connections. The continuation of growth of *P. wallichiana* withstanding different drought events indicates that the species is resilience to climate change, especially in dry environments. But, under the projected temperature rise for the 21st century, marginal communities like the Dolpo people who already live in a dry environment are likely to suffer more from extreme droughts.

Acknowledgments

This study was jointly supported by Yunnan Oriented Fund for Post Doctors, Climate Change Research Grant Program of PPCR Government of Nepal undertaken by Nepal Academy of Science and Technology with the support of Asian Development Bank (TA 7984-NEP), National Science Foundation of China (No. 31770533), National Key Research Development Program of China (2016YFC0502105), and the CAS 135 program (2017XTBG-T01). Authors are thankful to NAST for permission to use lab facilities, Department of National Park and Wildlife Conservation (DNPWC) for the permission to conduct this study in SPNP, and DHM for the meteorological data. Janak, LB Kathayat, and Ram P. Chaudhary, Warden of SPNP and their staff at Dolpa helped during fieldwork. Author SKS is thankful to Prof. S. Bajpai, Director of BSIP for providing permission to participate in this collaborative work with BSIP contribution number (BSIP/RDCC/74/2017-18). We are grateful to Professor Dr. James H. Speer, Indiana State University, USA for his valuable technical input and language editing in the final revised manuscript. The constructive comments given by anonymous reviewers and the editor helped us to improve the quality of our manuscript.

Appendix A. Supplementary data

Supplementary data to this article can be found online at https://doi.org/10.1016/j.palaeo.2018.10.026.

References

Agnew, C., 2000. Using the SPI to identify drought. Drought Network News 12 (1), 6–12.
Alley, W.M., 1984. The Palmer drought severity index: limitations and assumptions. J. Clim. Appl. Meteorol. 23, 1100–1109.
Aryal, S., Ghimire, S.K., Dhakal, Y.R., Gaire, N.P., Bhandari, S., 2017. Perceptions of agro-pastoralists towards the change in temperature and precipitation in the trans-Himalayan regions of Nepal. Banko Janakari 27 (1), 21–30.
Beach, T., Luzzadder-Beach, S., Dunning, N., Cook, D., 2016. Climatic changes and collapses in Maya history. PAGES Magazine 24 (2), 66–67. https://doi.org/10.22498/pages.24.2.66.
Bhattacharyya, A., Yadav, R.R., 1996. Dendrochronological reconnaissance of *Pinus wallichiana* to study glacial behaviour in the western Himalaya. Curr. Sci. 70 (8), 739–744.
Bhattacharyya, A., Lamarche Jr., V.C., Hughes, M.K., 1992. Tree ring chronologies from Nepal. Tree-Ring Bull. 52, 59–66.
Bhushan, R., Sati, S.P., Rana, N., Shukla, A.D., Mazumdar, A.S., Juyal, N., 2018. High resolution millennial and centennial scale Holocene monsoon variability in the Higher Central Himalayas. Palaeogeogr. Palaeoclimatol. Palaeoecol. 489, 95–104.
Böhner, J., Miehe, G., Miehe, S., Nagy, L., 2015. Climate and weather. In: Miehe, Georg, Pendry, Colin A., Chaudhary, Ram (Eds.), Nepal: An Introduction to the Natural History, Ecology and Human Environment of the Himalayas. Royal Botanic Garden, Edinburgh, pp. 385–472.
Borgaonkar, H.P., Ram, Somaru, Sikder, A.B., 2009. Assessment of tree–ring analysis of high–elevation *Cedrus deodara* D. Don from Western Himalaya (India) in relation to climate and glacier fluctuations. Dendrochronologia 27, 59–69.
Borgaonkar, H.P., Sikder, A.B., Ram, S., Pant, G.B., 2010. El Nino and related monsoon drought signals in 523–year–long ring width records of teak (*Tectona grandis* L.F.) trees from south India. Palaeogeogr. Palaeoclimatol. Palaeoecol. 285, 74–84.
Borgaonkar, H.P., Sikder, A.B., Ram, S., 2011. High altitude forest sensitivity to the recent warming: a tree–ring analysis of conifers from western Himalaya, India. Quat. Int. 236, 158–166. https://doi.org/10.1016/j.quaint.2010.01.016.
Bräuning, A., 2001. Climate history of the Tibetan Plateau during the last 1000 years derived from a network of Juniper chronologies. Dendrochronologia 19 (1), 127–137.
Bräuning, A., 2004. Tree–ring studies in the Dolpo–Himalaya (western Nepal). TRACE 2, 8–12.
Briffa, K.R., 1995. Interpreting high–resolution proxy climate data, the example of dendroclimatology. In: von Storch, H., Navarra, A. (Eds.), Analysis of Climate Data Variability, Applications of Statistical Techniques. Springer, New York, pp. 77–94.
Briffa, K.R., Melvin, T.M., 2009. A closer look at regional curve standardization of tree–ring records: justification of the need, a warning of some pitfalls, and suggested improvements in its application. In: Hughes, I.M.K., Diaz, H.F., Swetnam, T.W., Progress, D. (Eds.), Dendroclimatology: Progress and Prospects. Springer Verlag, New York City.
Buckley, B.M., Anchukaitis, K.J., Penny, D., Fletcher, R., Cook, E.R., Sano, M., Nam, L.C., Wichienkeeo, A., Minh, T.T., 2010. Climate as a contributing factor in the demise of Angkor, Cambodia. Proc. Natl. Acad. Sci. 107, 6748–6752.
Cai, Q., Liu, Y., Liu, H., Ren, J., 2015. Reconstruction of drought variability in North China and its association with sea surface temperature in the joining area of Asia and Indian–Pacific Ocean. Palaeogeogr. Palaeoclimatol. Palaeoecol. 417, 554–560.
Chen, F., Yuan, Y., Zhang, R., Qin, L., 2014. A tree–ring based drought reconstruction (AD 1760–2010) for the Loess Plateau and its possible driving mechanisms. Glob. Planet. Chang. 122, 82–88.
Cook, E.R., 1985. A Time–series Analysis Approach to Tree–ring Standardization. University of Arizona Press, Tucson (Ph.D. Dissertation).
Cook, E.R., Kairiukstis, A. (Eds.), 1990. Methods of Dendrochronology: Applications in the Environmental Sciences. Kluwer Academic Press, Dordrecht.
Cook, E.R., Krusic, P.J., Jones, P.D., 2003. Dendroclimatic signals in long tree–ring chronologies from the Himalayas of Nepal. Int. J. Climatol. 23, 707–732. https://doi.org/10.1002/joc.911.
Cook, E.R., Anchukaitis, K.J., Buckley, B.M., D'Arrigo, R., Jacoby, G.C., Wright, W.E., 2010. Asian monsoon failure and mega drought during the last millennium. Science

328, 486–489.
Dahal, P., Shrestha, N.S., Shrestha, M.L., Krakauer, N.Y., Panthi, J., Pradhanan, S.M., Jha, A., Lakhankar, T., 2016. Drought risk assessment in central Nepal: temporal and spatial analysis. Nat. Hazards 80, 1913–1932. https://doi.org/10.1007/s11069–015–2055–5.
Dai, A.G., Wigley, T.M.L., 2000. Global patterns of ENSO induced precipitation. Geophys. Res. Lett. 27, 1283–1286.
Dai, A., Trenberth, K.E., Qian, T., 2004. A global dataset of Palmer Drought Severity Index for 1870–2002: relationship with soil moisture and effects of surface warming. J. Hydrometeorol. 5, 1117–1130.
Dawadi, B., Liang, E., Tian, L., Devkota, L.P., Yao, T., 2013. Premonsoon precipitation signal in tree rings of timberline *Betula utilis* in the central Himalayas. Quat. Int. 283, 72–77. https://doi.org/10.1016/j.quaint.2012.05.039.
Devkota, A., 2013. Biodiversity: Gymnosperms. In: Jha, P.K., Neupane, F.P., Shrestha, M.L., Khanal, I.P. (Eds.), Biological Diversity and Conservation. Nepal Academy of Science and Technology, Kathmandu, pp. 127–134.
van der Schrier, G., Barichivich, J., Briffa, K.R., Jones, P.D., 2013. A scPDSI–based global data set of dry and wet spells for 1901–2009. J. Geophys. Res. Atmos. 118 (10), 4025–4048.
DHM, 2015. Study of Climate and Climatic Variation Over Nepal. Department of Hydrology and Meteorology, Ministry Of Science, Technology and Environment, Government of Nepal, Kathmandu, Nepal.
DNPWC, 2015. In: Dhakal, M. (Ed.), Protected Areas of Nepal. Department of National Park and Wildlife Conservation, Babarmal, Kathmandu, Nepal.
Dubey, B., Yadav, R.R., Singh, J., Chaturvedi, R., 2003. Upward shift of Himalayan pine in Western Himalaya, India. Curr. Sci. 85, 1135–1136.
Fan, Z.-X., Bräuning, A., Cao, K.-F., 2008. Tree ring based drought reconstruction in the central Hengduan Mountains region (China) since AD 1655. Int. J. Climatol. 28 (14), 1879–1887.
Fang, K., Gou, X., Chen, F., Li, J., D'Arrigo, R., Cook, E., Yang, T., Davi, N., 2010. Reconstructed droughts for the southeastern Tibetan Plateau over the past 568 years and its linkages to the Pacific and Atlantic Ocean climate variability. Clim. Dyn. 35 (4), 577–585.
Fang, K., Gou, X., Chen, F., Liu, C., Davi, N., Li, J., Zhao, Z., Li, Y., 2012. Tree–ring based reconstruction of drought variability (1615–2009) in the Kongtong Mountain area, northern China. Glob. Planet. Chang. 80–81, 190–197.
Farjon, A., 2011. "Pinus wallichiana". The IUCN Red List of Threatened Species. IUCN (e.T42427A2979371).
Fritts, H.C., 1976. Tree Rings and Climate. Cambridge University Press, Cambridge, pp. 567.
Gaire, N.P., Koirala, M., Bhuju, D.R., Borgaonkar, H.P., 2014. Treeline dynamics with climate change at the central Nepal Himalaya. Clim. Past 10, 1277–1290. https://doi.org/10.5194/cp–10–1277–2014.
Gaire, N.P., Bhuju, D.R., Koirala, M., Shah, S.K., Carrer, M., Timilsena, R., 2017. Tree-ring based spring precipitation reconstruction in western Nepal Himalaya since AD 1840. Dendrochronologia 42, 21–30.
Gou, X., Chen, F., Jacoby, G.C., Cook, E.R., Yang, M., Peng, J., Zhang, Y., 2007. Rapid tree growth with respect to the last 400 years in response to climate warming, north-eastern Tibetan Plateau. Int. J. Climatol. 27, 1497–1503.
Grissino–Mayer, H.D., 2001. Evaluating cross–dating accuracy: a manual and tutorial for the computer program COFECHA. Tree-Ring Res. 57, 205–221.
Holmes, R.L., 1983. Computer–assisted quality control in tree–ring dating and measurement. Tree-Ring Bull. 43, 69–78.
IPCC, 2014. Summary for policymakers. In: Climate Change 2014: Impacts, Adaptation, and Vulnerability. Part A: Global and Sectoral Aspects. Cambridge University Press, Cambridge, United Kingdom and New York, NY, USA, pp. 1–32 (Contribution of Working Group II to the Fifth Assessment Report of the Intergovernmental Panel on Climate Change [Field, C.B., V.R. Barros., D.J. Dokken., K.J. Mach., M.D. Mastrandrea.,T.E. Bilir., M. Chatterjee., K.L. Ebi., Y.O. Estrada., R.C. Genova., B. Girma., E.S. Kissel., A.N. Levy., S. MacCracken.,P.R. Mastrandrea., L.L. White., (eds.)]).
Kang, S., Yang, B., Qin, C., Wang, J., Shi, F., Liu, J., 2013. Extreme drought events in the years 1877–1878, and 1928, in the southeast Qilian Mountains and the air–sea coupling system. Quat. Int. 283, 85–92.
Kansakar, S.R., Hannah, D.M., Gerrard, J., Rees, G., 2004. Spatial pattern in the precipitation regime of Nepal. Int. J. Climatol. 24, 1645–1659. https://doi.org/10.1002/joc.1098.
Karki, R., Hasson, S., Schickhoff, U., Scholten, T., Böhner, J., 2017. Rising precipitation extremes across Nepal. Climate 5, 4. https://doi.org/10.3390/cli5010004.
Kharal, D.K., Thapa, U.K., George, S., Meilby, H., Rayamajhi, S., Bhuju, D.R., 2017. Tree–climate relations along an elevational transect in Manang Valley, central Nepal. Dendrochronologia 41, 57–64. https://doi.org/10.1016/j.dendro.2016.04.004.
Kharel–Kafle, H., 2014. Spatial and temporal variation of drought in far and Mid–Western Regions of Nepal: time series analysis (1982–2012). Nepal J. Sci. Technol. 15 (2), 65–76.
Li, J.B., Gou, X.H., Cook, E.R., Chen, F.H., 2006. Tree–ring based drought reconstruction for the central Tien Shan area in Northwest China. Geophys. Res. Lett. 33, L07715.
Li, J., Chen, F., Cook, E.R., Gou, X., Zhang, Y., 2007. Drought reconstruction for north central China from tree–rings: the value of the Palmer drought severity index. Int. J. Climatol. 27, 903–909.
Liang, E., Shao, X.M., Xu, Y., 2009. Tree–ring evidence of recent abnormal warming on the southeast Tibetan Plateau. Theor. Appl. Climatol. 98, 9–18.
Liang, E.Y., Dawadi, B., Pederson, N., Eckstein, D., 2014. Is the growth of birch at the upper timberline in the Himalayas limited by moisture or by temperature? Ecology 95, 2453–2465.
Lu, R., Gao, S., Wang, Y., Ma, Y., Qiang, M., Zhang, D., 2013. Tree–ring based drought reconstruction at the northwestern margin of monsoon region of China since 1862. Quat. Int. 283, 93–97.
Mann, M.E., Lees, J., 1996. Robust estimation of background noise and signal detection in climate time series. Climate Change 33, 409–445.
McChesney, K., 2015. Existential avalanche the lived experience of climate change in Dolpo and Mustang, Nepal. In: Independent Study Project (ISP) Collection. Paper 2091, . http://digitalcollections.sit.edu/isp_collection/2091.
Meko, D.M., Graybill, D.A., 1995. Tree–ring reconstruction of upper Gila River discharge. J. Am. Water Resour. Assoc. 31, 605–616.
Melvin, T.M., Briffa, K.R., 2008. A signal–free approach to dendroclimatic standardization. Dendrochronologia 26 (2), 71–86.
Michaelsen, J., 1987. Cross-validation in statistical climate forecast models. J. Clim. Appl. Meteorol. 26, 1589–1600.
Miehe, G., Miehe, S., Böhner, J., Bäumler, R., Ghimire, S.K., Bhattarai, K., Chaudhary, R.P., Subedi, M., Jha, P.K., Pendry, C., 2015. Vegetation ecology. In: Miehe, Georg, Pendry, Colin A., Chaudhary, Ram (Eds.), Nepal: An Introduction to the Natural History, Ecology and Human Environment of the Himalayas. Royal Botanic Garden, Edinburgh, pp. 385–472.
MOE, 2010. National Adaptation Programme of Action to Climate Change. Ministry of Environment, Kathmandu, Nepal.
Palmer, W.C., 1965. Meteorological drought. In: Weather Bureau Research Paper 45. United States Department of Commerce, Washington DC.
Panday, P.K., Thibeault, J., Frey, K.E., 2015. Changing temperature and precipitation extremes in the Hindu Kush–Himalayan region: an analysis of CMIP3 and CMIP5 simulations and projections. Int. J. Climatol. 35 (10), 3058–3077. https://doi.org/10.1002/joc.4192.
Panthi, S., Bräuning, A., Zhou, Z.-K., Fan, Z.-X., 2017. Tree rings reveal recent intensified spring drought in the Central Himalaya, Nepal. Glob. Planet. Chang. 157, 26–34. https://doi.org/10.1016/j.gloplacha.2017.08.012.
Pederson, N., Hessl, A.E., Baatarbileg, N., Anchukaitis, K.J., Cosmo, N.D., 2014. Pluvials, droughts, the Mongol Empire, and modern Mongolia. PNAS 111 (12), 4375–4379. https://doi.org/10.1073/pnas.1318677111.
Peng, J.F., Liu, Y.Z., 2013. Reconstructed droughts for the northeastern Tibetan Plateau since AD 1411 and its linkages to the Pacific, Indian and Atlantic Oceans. Quat. Int. 283, 98–106.
Ram, S., 2012. Tree growth–climate relationships of conifer trees and reconstruction of summer season Palmer Drought Severity Index (PDSI) at Pahalgam in Srinagar, India. Quat. Int. 254, 152–158.
Rinn, F., 2003. TSAP–Win: time series analysis and presentation for dendrochronology and related applications. Version 0.55 User reference. Heidelberg, Germany. Available at. http://www.rimatech.comSalzer.
Saji, N.H., Yamagata, T., 2003. Possible impacts of Indian Ocean Dipole mode events on global climate. Clim. Res. 25, 151–169.
Sano, M., Furuta, F., Kobayashi, O., Sweda, T., 2005. Temperature variations since the mid–18th century for western Nepal, as reconstructed from tree–ring width and density of *Abies spectabilis*. Dendrochronologia 23, 83–92. https://doi.org/10.1016/j.dendro.2005.08.003.
Sano, M., Ramesh, R., Sheshshayee, M.S., Sukumar, R., 2012. Increasing aridity over the past 223 years in Nepal Himalaya inferred from a tree ring δ18O chronology. The Holocene 22 (7), 809–817.
Schmidt, B., Wazny, T., Malla, K., Höfs, E., Khalessi, M., 1999. Chronologies for historical dating in high Asia/Nepal. In: Wimmer, R., Vetter, R.E. (Eds.), Tree ring Analysis: Biological, Methodological, and Environmental Aspects. CABI Publishing, Oxon, United Kingdom, pp. 205–211.
Shah, S.K., Bhattacharyya, A., 2012. Spatio-temporal growth variability three Pinus species of Northeast Himalaya with relation to climate. Dendrochronologia 30, 266–278.
Shrestha, H.K., Prasain, S., 2016. Climate change impact and adaptation measures needed in upper Mustang to prevent more climate refugees. In: Bhuju, D.R., McLaughlin, K., Sijapati, J., Devkota, B.D., Shrestha, N., Ghimire, G.P., Neupane, P.K. (Eds.), Building Knowledge for Climate Resilience in Nepal: Research Briefs. Nepal Academy of Science and Technology, Khumaltar, Lalitpur, pp. 125–129.
Shrestha, A.B., Wake, C.A., Mayewski, P.A., Dibb, J.E., 1999. Maximum temperature trends in the Himalaya and its vicinity: an analysis based on temperature records from Nepal for the period 1971–94. J. Clim. 12, 2775–2786.
Shrestha, U.B., Gautam, S., Bawa, K.S., 2012. Widespread climate change in the Himalayas and associated changes in local ecosystems. PLoS One 7, e36741. https://doi.org/10.1371/journal.pone.0036741,2012.
Shrestha, K.B., Hofgaard, A., Vandvik, V., 2015. Recent treeline dynamics are similar between dry and mesic areas of Nepal, central Himalaya. J. Plant Ecol. 8 (4), 347–358. https://doi.org/10.1093/jpe/rtu035.
Sigdel, M., Ikeda, M., 2010. Spatial and temporal analysis of drought in Nepal using Standardized Precipitation Index and its relationship with climate indices. J. Hydrol. Meteorol. 7 (1), 59–74.
Singh, J., Yadav, R.R., 2000. Tree–ring indications of recent glacier fluctuations in Gangotri, Western Himalaya, India. Curr. Sci. 79, 1598–1601.
Singh, J., Yadav, R.R., Wilmking, M., 2009. A 694-year tree-ring based rainfall reconstruction from Himachal Pradesh, India. Clim. Dyn. 33, 1149–1158.
Snee, R.D., 1997. Validation of regression models: methods and examples. Technometrics 19, 415–428.
Song, H.M., Liu, Y., 2011. PDSI variations at Kongtong Mountain, China, inferred from a 283–year *Pinus tabulaeformis* ring–width chronology. J. Geophys. Res. 116, D22111. https://doi.org/10.1029/2011JD016220.
Speer, J.H., 2010. Fundamentals of Tree Ring Research. The University of Arizona Press, Tucson.
Stainton, J.D.A., 1972. Forests of Nepal. The Camelot Press Limited, Southampton,

London, UK.
Sun, J., Liu, Y., 2013. Drought variations in the middle Qilian Mountains, northeast Tibetan Plateau, over the last 450 years as reconstructed from tree rings. Dendrochronologia 31, 279–285.
Thapa, U.K., Shah, S.K., Gaire, N.P., Bhuju, D.R., 2015. Spring temperatures in the far–western Nepal Himalaya since AD 1640 reconstructed from *Picea smithiana* tree–ring widths. Clim. Dyn. 45 (7–8), 2069–2081. https://doi.org/10.1007/s00382-014-2457-1.
Thapa, U.K., St.George, S., Kharal, D.K., Gaire, N.P., 2017. Tree growth across the Nepal Himalaya during the last four centuries. Prog. Phys. Geogr. 1–18. https://doi.org/10.1177/0309133317714247.
Trouet, V., Oldenborgh, G.J.V., 2013. KNMI climate explorer: a web based research tool for high–resolution paleoclimatology. Tree-Ring Res. 69 (1), 3–13.
Wang, X.C., Zhang, Q.B., Ma, K.P., Xiao, S.C., 2008. A tree ring record of 500-year dry wet changes in northern Tibet, China. The Holocene 18 (4), 579–588.
Wang, S.Y., Yoon, J.H., Gillies, R.R., Cho, C., 2013. What caused the winter drought in Western Nepal during recent years? J. Clim. 26, 8241–8256. https://doi.org/10.1175/JCLI–D–12–00800.1.
Webster, P.J., Yang, S., 1992. Monsoon and ENSO: selectively interactive systems. Q. J. R. Meteorol. Soc. 118, 877–926.
Weisberg, S., 1985. Applied Linear Regression. John Wiley, New York (324 pp).
Weiss, H., 2016. Global megadrought, societal collapse and resilience at 4.2–3.9 ka BP across the Mediterranean and west Asia. PAGES Magazine 24 (2), 62–63. https://doi.org/10.22498/pages.24.2.62.
Weiss, H., Bradley, R.S., 2001. Archaeology–what drives societal collapse? Science 291, 609–610.
Wigley, T.M.L., Briffa, K.R., Jones, P.D., 1984. On the average value of correlated time series, with applications in dendroclimatology and hydrometeorology. J. Clim. Appl. Meteorol. 23, 201–213.
Xu, J., Grumbine, R.E., Shrestha, A., Eriksson, M., Yang, X., Wang, Y., Wilkes, A., 2009. The melting Himalayas: cascading effects of climate change on water, biodiversity, and livelihoods. Conserv. Biol. 23, 520–530. https://doi.org/10.1111/j.1523–1739.2009.01237.x.
Yadav, R.R., 2009. Tree ring imprints of long-term changes in climate in western Himalaya, India. J. Biosci. 34 (5), 699–707. https://doi.org/10.1007/s12038-009-0058-7.
Yadav, R.R., 2013. Tree ring–based seven–century drought records for the Western Himalaya, India. J. Geophys. Res. Atmos. 118 (10), 4318–4325. https://doi.org/10.1002/jgrd.50265.
Yadav, R.R., Mishra, K.G., Kotila, B., Upreti, N., 2014. Premonsoon precipitation variability in Kumaon Himalaya, India over a perspective of ~300 years. Quat. Int. 325, 213–219.
Yadava, A.K., Bräuning, A., Singh, J., Yadav, R.R., 2016. Boreal spring precipitation variability in cold arid western Himalaya during the last millennium and its relationship with hydrological records and human history. Quat. Sci. Rev. 144, 28–43.
Zurick, D., Pacheco, J., Shrestha, B., Bajracharya, B. (Eds.), 2005. Atlas of the Himalaya, ICIMOD, Kathmandu, Nepal.